Reports

San Simeon–Hosgri Fault System, Coastal California: Economic and Environmental Implications

Abstract. *There has been 80 kilometers or more of right slip along the late Quaternary San Simeon–Hosgri fault system of coastal California during the last 5 to 13 million years. Part of an oil-rich basin is probably offset by this fault system, and the system may be a potential hazard to nearby structures.*

Comparison of stratigraphic sections exposed on opposite sides of the late Quaternary San Simeon–Hosgri fault system at Point Sal and near San Simeon (Fig. 1) strongly suggests large-scale lateral displacement. The nature and age of strike-slip displacement along the fault system has important economic and environmental implications, for it suggests the possible location of an offshore extension of the oil-producing Santa Maria basin and indicates that the system poses a potential hazard to engineered facilities.

The San Simeon fault in coastal central California, first named in 1974 (*1*), can be traced on land for a distance of approximately 19 km—that is, from Ragged Point to San Simeon Point (Fig. 2). In the area offshore from Ragged Point, Hoskins and Griffiths (*2*) show a 65-km northwestward extension of the San Simeon fault. Silver (*3*) reports a fault with as much as 5 km of dip separation in the offshore basin south of Point Sur (that is, 80 km north of San Simeon), which may be the northern extension of the San Simeon fault. The San Simeon fault may also extend farther south from San Simeon Point to near Point Estero (Fig. 1) in the offshore, as postulated by others (*1*). Such a suggestion is supported by the fact that the coastline is straight and rises abruptly from the sea.

Near San Simeon Point the trace of the San Simeon fault is concealed by late Pleistocene or Holocene slightly cemented dune sand deposits. It faults the 122-m Pleistocene terrace approximately 5 km northeast of Point Piedras Blancas, but does not cut the 12-m terrace near either Breaker Point or Ragged Point.

The Arroyo Laguna fault (Fig. 2) is believed to be a relatively younger and more recently active strand of the San Simeon fault zone. This fault is marked by a pronounced linear valley north of San Simeon Point (*4*), by a 75-m fault scarp, and by faulting of the 122-m Pleistocene terrace. The fault crosses several west- or southwest-draining canyons, including Arroyo Hondo, Arroyo de los Chinos, and three other unnamed canyons between Arroyo de los Chinos and Arroyo de la Cruz (*4*). Each canyon is marked by right lateral deviation of 150 to 450 m; however, the fault does not juxtapose markedly different rock sequences or types (Fig. 2) as does the San Simeon fault.

The San Simeon fault terminates the Arroyo del Oso fault, which cuts through the lower part of the 12-m terrace (*1, 4*). The Pleistocene terrace deposits within the region are 130,000 ± 30,000 and 140,000 ± 20,000 years old (*5*); therefore the Arroyo del Oso fault is younger than approximately 130,000 years and, at least in part, the San Simeon fault must be still younger. An epicenter (date unrecorded) is located on the Arroyo del Oso fault and the magnitude of the earthquake is reported to have been between 4.0 and 4.4 (*6*). Holden (*7*) reports earthquakes of 26 October or 26 November 1852 and 1 February 1853 at San Simeon, where "houses were injured." However, the authenticity of these early

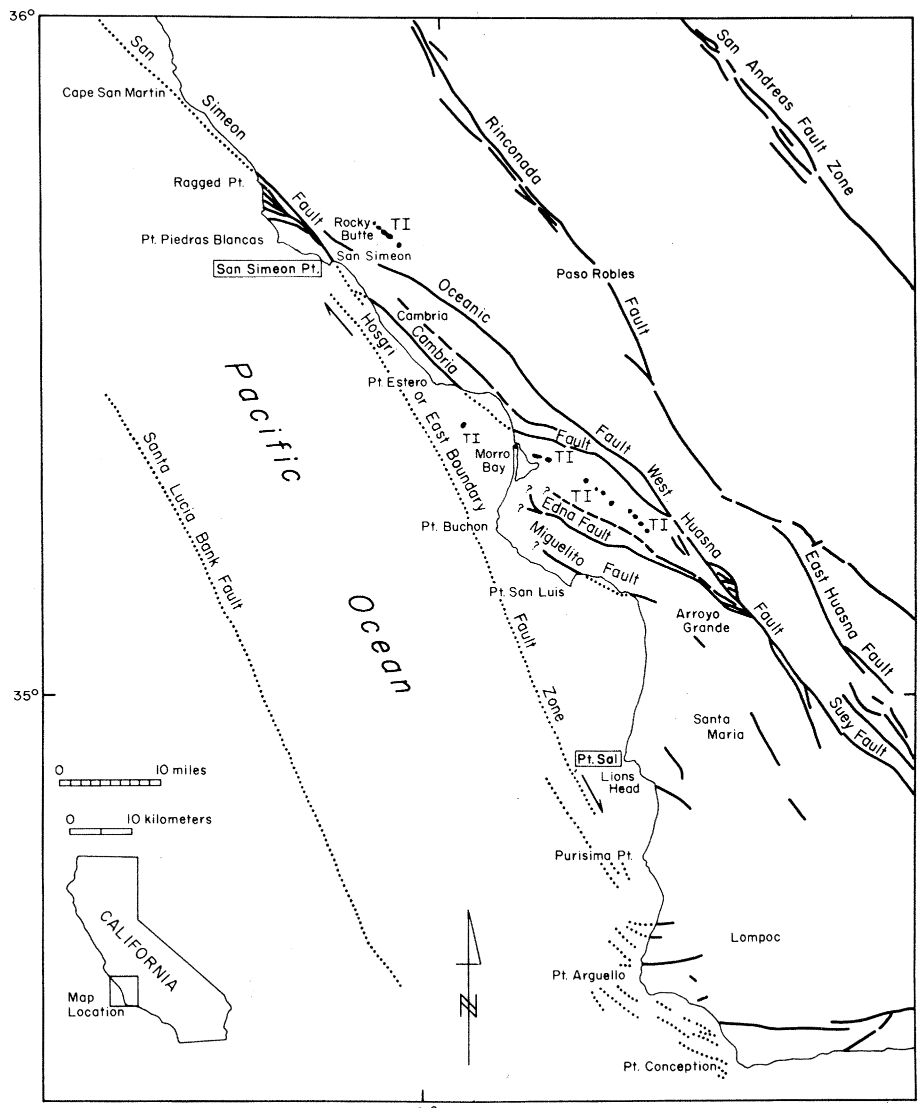

Fig. 1. Location of the San Simeon–Hosgri fault system. Base map is from Jennings (*11*) and several other sources (*1, 2, 4, 9, 10, 13*). Spots indicate hypabyssal plugs of the Morro Rock–Islay Hill complex (*1, 10, 17*).

earthquake reports has been questioned (*8*).

The San Simeon fault terminates the Oceanic–West Huasna–Suey fault system (Fig. 1). The West Huasna fault may terminate the Edna fault (*9*), which in turn displaces Pleistocene and late Pleistocene deposits (*9*). Thus, although movement began earlier, probably between the late Miocene and late Pliocene, the San Simeon fault must be Pleistocene or younger, and strands or associated faults may be even younger.

The Hosgri fault (*10*), also called the East Boundary fault or fault zone (*1*), extends southeastward from near Point Piedras Blancas to near Point Sal, but south of Point Sal the continuation is not clear (*11*). Seismic reflection records (*1, 10*) show that there has been dip separation, with the west side moving down relative to the east side. Differential movement has occurred intermittently along the Hosgri fault from late Miocene to Holocene time (*1*). Earthquake epicenters along the fault suggest that it could be seismically active (*1, 10, 12*). Arguments supporting and refuting the possibility of strike-slip movement along the Hosgri fault have been carefully reviewed (*1*); however, new data presented here strongly suggest that the San Simeon and Hosgri faults are part of the same system, right slip accounting for the distribution of Jurassic to Pliocene rocks.

Recent geologic mapping near San Simeon (*4*) and the area between Santa Maria and San Simeon (*9, 13*) (Figs. 1 and 2) has shown that remarkable similarities exist between rocks west of the San Simeon fault zone, near San Simeon, and east of the Hosgri fault near Point Sal (Fig. 1). Jurassic ophiolite, overlain successively by tuffaceous radiolarian chert and Jurassic shale; Oligocene nonmarine conglomerate, associated tuff, and distinctive landslide deposits; and later Tertiary cherty shale of similar composition and histories are offset (Fig. 3). The horizontal slip component may be 80 km or more.

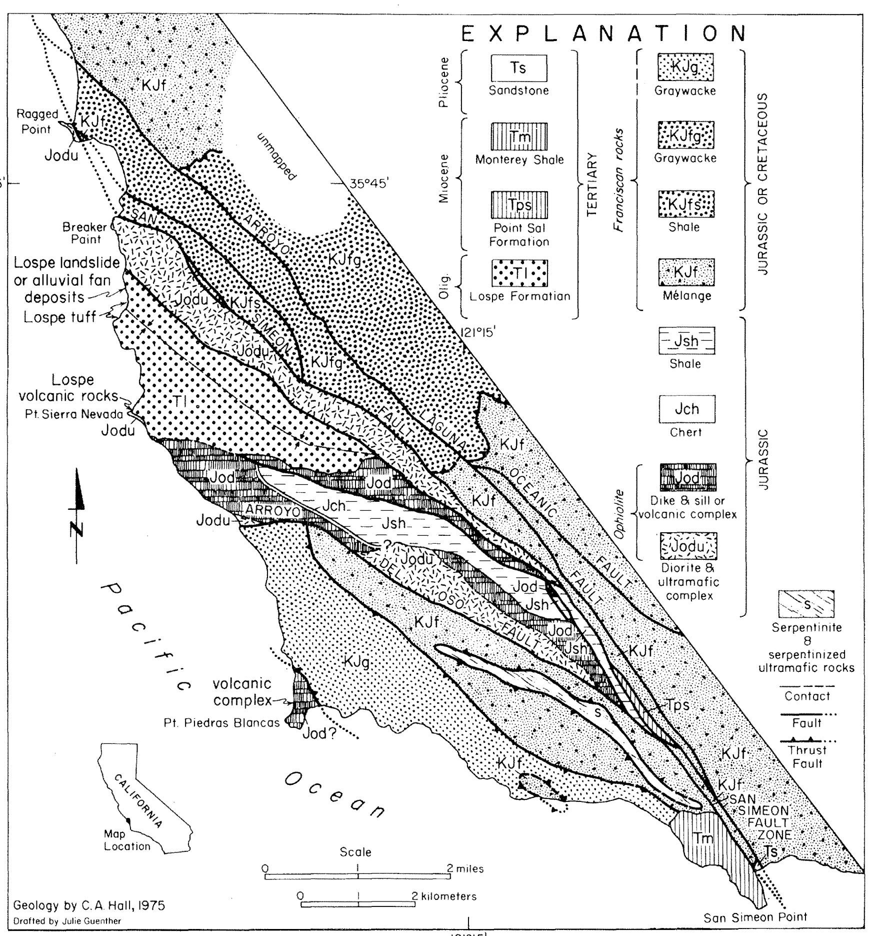

Fig. 2. Pre-Quaternary geologic map showing distribution and stratigraphic relations of the Jurassic ophiolite, chert, and shale sequence; the Oligocene Lospe Formation; and Monterey Shale near San Simeon, California (*4*). This map should be compared with geologic maps of the Point Sal–Lions Head area (*14, 15*), where the Lospe Formation overlies the Jurassic ophiolite and shale. The rocks in the San Simeon Point area would have been at least 12 km offshore from Point Sal prior to movement along the San Simeon–Hosgri fault system.

The rocks in the Point Sal area have been described by Woodring and Bramlette (*14*) and, more recently, the ophiolite has been described by Hopson *et al.* (*15*). The oldest rocks in that area are those of the Jurassic (~160 million years) ophiolite, which consists of a lower part of serpentinite, layered ultramafic rocks, and gabbro; and an upper part of diorite, quartz diorite, a dike and sill complex, and submarine pillow lavas. Greenish-gray tuffaceous radiolarian chert, overlain by Jurassic shale and sandstone, rests on the ophiolite complex (*15*). A similar sequence of rocks occurs north of San Simeon (Fig. 2) between the Arroyo del Oso and San Simeon faults, but the lower part of the complex present near Point Sal is apparently absent, as are the submarine lavas, in the San Simeon area.

A Jurassic ophiolite east of Morro Bay (*13, 16*), east of the San Simeon fault, and in relatively close proximity to San Simeon, is overlain by red radiolarian chert, not the distinctive greenish-gray tuffaceous chert west of the San Simeon fault.

The Franciscan shale (Fig. 2) in the San Simeon area consists of dark greenish-gray and brown weathering clay shale. The unit is lithologically similar to the Honda Formation of Dibblee (*17*) south of Point Sal, but it is not recognized in the Santa Maria area; it is presumed to lie within the fault block northeast of the San Simeon fault.

Jurassic shale in the San Simeon area is lithologically similar to the Knoxville Formation (*14*) in the Santa Maria area and the Espada Formation of Dibblee (*17*) farther south. In both the Point Sal and San Simeon areas the Jurassic shale contains beds of conglomerate consisting of well-rounded, smooth, small, black chert pebbles.

Stratigraphically above the Jurassic ophiolite-chert-shale sequence in both the San Simeon and Point Sal areas is the Lospe Formation (Fig. 2), a nonmarine rock unit consisting chiefly of reddish conglomerate and coarse-grained sandstone and tuff overlain by greenish sandstone and tuff (*14*). In the Point Sal area the Lospe Formation (*14, 15*) of Oligocene age overlaps Jurassic shale and rests on the ophiolite complex. In the San Simeon area similar stratigraphic relationships are complicated by faulting (Fig. 2). The greenish sandstone is not well developed near San Simeon. In both the Point Sal and San Simeon areas the conglomerate is unsorted and poorly stratified. Clasts range in size from a few inches to several feet in diameter and consist of rocks from the ophiolite complex and lesser amounts of Jurassic chert and shale. Nowhere in the

Lospe Formation west of the San Simeon fault (Fig. 2) are there clasts of dacite or felsite from the 22-million- to 26-million-year-old Morro Rock–Islay Hill complex (*9, 13, 18*), the dacite of Rocky Butte (*Tl* in Fig. 1), or the Cambria Felsite (*9, 18*). Dacite and felsite clasts are not present in the Lospe Formation in the Point Sal region. However, clasts of these rocks are present in the Lospe and Oligocene and lower Miocene rocks only a few kilometers east of San Simeon (*9*) and near Cambria. Thus, the inference is made that Lospe strata west of the San Simeon fault zone were not in the Cambria area at the time of their deposition. Clasts of dacite and Cambria Felsite are present only in Pleistocene and younger deposits west of the San Simeon fault (*4*).

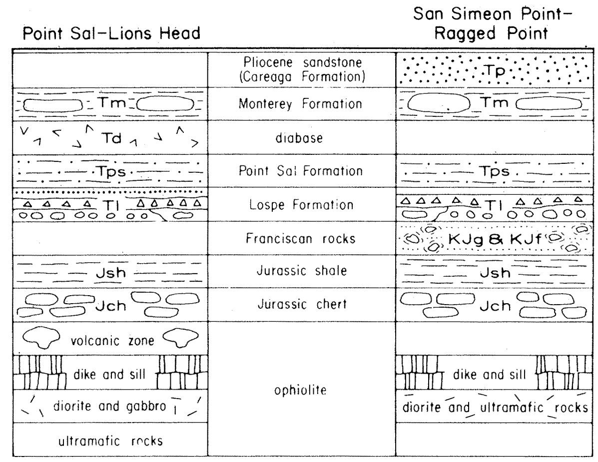

Fig. 3. Pre-Quaternary composite stratigraphic sections of rocks in the Point Sal–Lions Head area, Santa Barbara County (*14, 15*), and the San Simeon Point–Ragged Point area, San Luis Obispo County (*4*).

There are volcanic ash or tuff deposits within the Lospe Formation at both the Point Sal and San Simeon localities. At Point Sal the tuff occurs near the base of the conglomerate and near the middle of the Lospe Formation (*14*); north of San Simeon it occurs above conglomerate. South of Point Sal, near Lions Head, a landslide occurs within the Lospe Formation below a prominent white tuff bed (*14*). South of Breaker Point (Fig. 2) a large Oligocene landslide or alluvial fan also lies immediately below tuff and other volcanic rocks within the Lospe Formation. Here clasts in the Lospe landslide are more variable in size and lithology than those in the Lospe landslide south of Point Sal; however, at both localities the clasts are predominantly serpentinite, gabbro, diorite, and basaltic rocks. The occurrence of distinctive landslides or landslide-like deposits immediately below a tuff bed in the same formation at two widely separated localities on opposite sides of the San Simeon–Hosgri fault system strongly argues for their preslip contiguity.

In addition to the remarkable similarities between rock types, structural styles, and stratigraphic relationships of the diorite and dike and sill complex within the ophiolite and to the presence of the Lospe Formation near Point Sal and San Simeon, there is an extraordinary resemblance between the lithologies of the middle or upper part of the Monterey Shale at these two areas. In both regions and east and west of the San Simeon fault there is thin-bedded cherty shale—a characteristic of the Monterey Shale. However, west of the San Simeon fault, approximately 2 km northwest of San Simeon Point (Fig. 2), 0.3- to 1-m-thick beds of black chert interbedded with diatomaceous siltstone are also present. South of Point Sal, near Lions Head, identical lithologies occur (*14*). However, in the several hundred square kilometers that have been mapped east of the San Simeon fault and northwest of Santa Maria (*9, 13*) thick black chert beds are not present.

A small outcrop probably of Pliocene age has been mapped near San Simeon (Fig. 2) within the San Simeon fault zone. The outcrop contains marine fossils: *Dendraster* sp., bryozoa, *Dentalium* sp., *Solen* sp., and *Nuculana (Saccella) taphria* (Dall, 1897). The fossils do not date the rocks more precisely than early Pliocene to Holocene. The lithology, however, is similar to that of the Graciosa Coarse-Grained Member of the Careaga Sandstone in the Santa Maria area (*14*).

On the whole, strong stratigraphic and lithologic similarities exist between two packages of five or six lithologic units exposed in the San Simeon and Point Sal areas. The diameters of these relatively unique lithologic packages are estimated at not more than 20 km each (*4, 9, 13–15, 19*). Rock sequences within a radius of 20 to 100 km to the east of San Simeon are unlike those west of the San Simeon fault.

Comparison of the stratigraphic and lithologic histories of the areas near Point Sal and San Simeon (Fig. 1), areas that lie on opposite sides of the San Simeon–Hosgri fault system, indicates strong evidence for right slip of 80 or more kilometers along the fault system since the late Miocene or early Pliocene. It is assumed that separation is equal to or nearly equal to the horizontal slip component. The uncertainties of determining the minimum horizontal slip component are equal to the uncertainties, in one direction, of the maximum size of the area of the stratigraphic packages. Thus, the horizontal slip component is calculated to be 80 km or more (that is, more than 100 km between Point Sal and San Simeon Point, minus the estimated maximum 20-km diameter of the area of the stratigraphic packages at San Simeon and Point Sal).

If the conclusion is correct, then there are at least three significant corollaries.

1) The rate of motion between the Pacific and North American plates, between 4.5 and 10 million years ago, averaged 4.5 cm/year according to Atwater and Molnar (*20*). Therefore, 450 km of displacement would have taken place within the last 10 million years. This calculated amount exceeds right slip measured along the San Andreas fault by 150 km (*21*) during the last 10 to 12 million years. Some of the relative motion, 80 km in 5 million to 13 million years, may have been taken up or absorbed in the Salinia block or—as suggested here—offshore along the San Simeon–Hosgri fault system.

2) The Santa Maria basin contains several producing oil fields (*19*). A thickness of 300 m to 4 km of Cenozoic sedimentary rocks is present offshore from the San Simeon area (*1–3*) and would be part of the Santa Maria basin that has been displaced northward along the San Simeon–Hosgri fault system. Instead of simple westward projection of that part of the Santa Maria basin, which is currently producing commercial quantities of hydrocarbons, an 80-km northwest projection might be more valid.

3) The late Quaternary San Simeon–Hosgri fault system could be a potential hazard to any engineered structure located along the coast from San Simeon south to the vicinity of Purisima Point (Fig. 1).

C. A. Hall Jr.

Department of Geology,
University of California,
Los Angeles 90024

References and Notes

1. Earth Science Associates (Palo Alto, Calif.), "Geology of the southern Coast Ranges and the adjoining offshore continental margin of California, with special reference to the geology in the vicinity of the San Luis Range and Estero Bay," report for Pacific Gas and Electric Company to establish potential for seismic activity that could affect Diablo Canyon Nuclear Power Plant (1974).
2. E. G. Hoskins and J. R. Griffiths, *Am. Assoc. Pet. Geol. Mem.* **15**, 212 (1971).

3. E. A. Silver, *San Joaquin Geol. Soc. Short Course* (1974), p. 6-1.
4. C. A. Hall Jr., Geologic map of the Piedras Blancas–San Simeon region, California, in preparation.
5. H. H. Veeb and J. W. Valentine, *Geol. Soc. Am. Bull.* **78**, 547 (1968).
6. *Calif. Dep. Water Resour. Bull. 116-2* (1964).
7. E. S. Holden, *Smithson. Misc. Collect. 1087* (1897).
8. P. Squibb, personal communication. Mr. Squibb is past president of the San Luis Obispo County Historical Society.
9. C. A. Hall Jr., *Geol. Soc. Am. Bull.* **78**, 559 (1967); *Calif. Div. Mines Geol. Map Sheet* (1973); *U.S. Geol. Surv. Misc. Field Stud. Map MF-511* (1973); *U.S. Geol. Surv. Misc. Field Stud. Map MF-599* (1974); D. L. Turner, *Geol. Soc. Am. Spec. Pap. 124* (1970), p. 91; D. L. Turner, R. C. Surdam, C. A. Hall, *Geol. Soc. Am. Abstr. Cordilleran Sect.* **2**, 155 (1970).
10. H. C. Wagner, *U.S. Geol. Surv. Open File Rep. 74-252* (1974).
11. C. W. Jennings, *Calif. Div. Mines Geol. Prelim. Rep. 13* (1973).
12. W. Gawthrop, *U.S. Geol. Surv. Open File Rep. 75-134* (1975).
13. C. A. Hall Jr., "Geologic map of the Cayucos–San Luis Obispo region," *U.S. Geol. Surv., Misc. Field Stud. Map*, in press.
14. W. P. Woodring and M. N. Bramlette, *U.S. Geol. Surv. Prof. Pap. 222* (1950).
15. C. A. Hopson, C. J. Frano, E. A. Pessagno, Jr., J. M. Mattinson, "Preliminary report and geologic guide to the Jurassic ophiolite near Point Sal, Southern California coast," *Geol. Soc. Am. Cordilleran Sect. Guideb. Field Trip No. 5* (March 1975).
16. B. M. Page, *Geol. Soc. Am. Bull.* **83**, 957 (1972).
17. T. W. Dibblee Jr., *Calif. Div. Mines Bull. 150* (1950).
18. W. G. Ernst and C. A. Hall Jr., *Geol. Soc. Am. Bull.* **85**, 523 (1974).
19. Pacific Section, American Association of Petroleum Geologists, *Correlation Section across Santa Maria Basin 12* (1959).
20. T. Atwater and P. Molnar, *Stanford Univ. Publ. 13* (1973), p. 136.
21. O. F. Huffman, *Geol. Soc. Am. Bull.* **83**, 2913 (1972).

22. Publication approved by the director, U.S. Geological Survey. I thank W. G. Ernst, G. Oertel, E. Pampeyan, and H. Wagner for their constructive comments. J. Guenther and V. Jones drafted the figures. Research supported by the U.S. Geological Survey, the Nuclear Regulatory Commission, and the University of California Research Committee.

29 August 1975; revised 14 October 1975

Stratospheric Ozone: The Possible Effects of Tropospheric-Stratospheric Feedback

Abstract. *The existence of tropospheric-stratospheric feedback mechanisms affecting variations in stratospheric ozone indicates the need to model the complete tropospheric-stratospheric system. For instance, a decrease in stratospheric ozone results in increased photolytic destruction of nitrous oxide in the troposphere and thereby reduced production of nitric oxide in the stratosphere. Estimates indicate that this mechanism will result in a recovery in atmospheric ozone of about 6 to 13 percent of the initial perturbation.*

As a result of recent studies, the prediction has been made that the release of stratospheric pollutants, such as nitrogen oxides, NO_x, from supersonic transports and ClX (Cl, ClO, HCl) from the photolytic destruction of chlorofluoromethanes will cause a significant diminution in the atmospheric O_3 content (*1–3*). In order to quantitatively assess the effects of these and other perturbations, several photochemical models have been constructed (*2, 4, 5*). In these models it is generally assumed, as a lower boundary condition, that the tropospheric mixing ratios of long-lived gases, such as N_2O, CH_4, and CH_3Cl, are constant and do not vary with changes in the O_3 column above (*2, 4, 5*). This practice effectively decouples the tropospheric-stratospheric system, not allowing for possible feedback between the troposphere and stratosphere. In fact, it is likely that a perturbation in the stratospheric O_3 content will, because of the resultant change in near-ultraviolet radiation penetrating the tropopause, cause changes in tropospheric photochemistry.

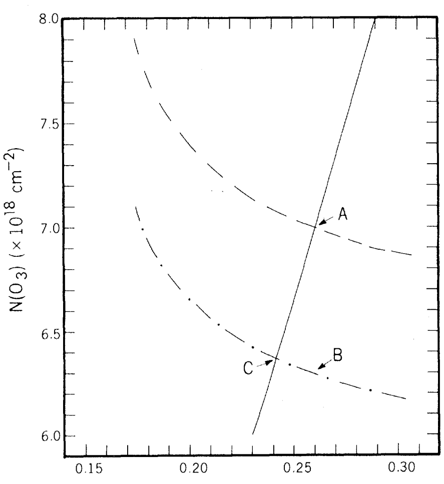

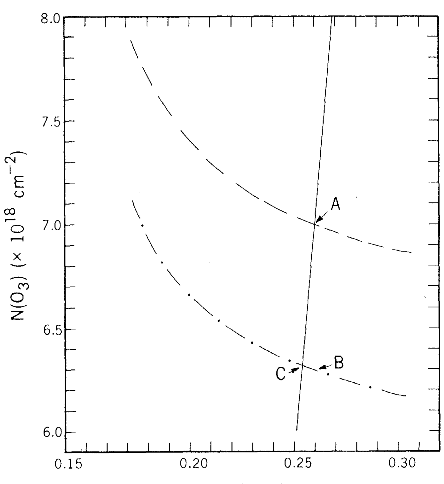

Fig. 1 (left). Results for case I. The solid line represents the dependence of X, the tropospheric N_2O mixing ratio, upon $N(O_3)$, the O_3 column above 15 km. The dashed line represents the dependence of $N(O_3)$ upon X after Crutzen (*9*). The dashed-dotted line represents the dependence of $N(O_3)$ upon X with an assumed uniform 10 percent perturbation. Under present-day conditions, the coupled system is in equilibrium at *A*. The initial effect of an assumed 10 percent perturbation would be to move the system from *A* to *B*. Equilibrium is reestablished at *C*, reducing the effect of the perturbation. Fig. 2 (right). Results for case II. For an explanation of the abbreviations used, see the legend to Fig. 1.

Calculations, based on a model similar to that of Chameides (*6*), indicate that a 10 percent decrease in the O_3 column above 15 km, $N(O_3)$, results in an approximate 13 percent increase in the photolytic destruction rate of N_2O and a 20 percent increase in the tropospheric concentration of OH radicals. These increases will cause a decrease in the tropospheric concentration of N_2O, and in the concentration of CH_4 and CH_3Cl, both of which are destroyed by OH (*7*). Thus a decrease in $N(O_3)$ may result in a decrease in the tropospheric input of NO_x, CH_4, H_2O, odd hydrogen (OH, HO_2, H_2O_2, H), and ClX to the stratosphere, possibly leading to feedback effects.

We estimate that these feedback effects are small but not insignificant, an indication that the entire tropospheric-stratospheric system must be modeled. The largest of the tropospheric feedback mechanisms that we have identified thus far involves tropospheric N_2O and is discussed below.

The major source of stratospheric NO_x is the oxidation of N_2O (*8*) by excited oxygen atoms: $O(^1D) + N_2O \rightarrow 2NO$. Since catalytic destruction by NO_x is the major sink of stratospheric O_3 (*1*), the stratospheric abundance of N_2O plays a major role in determining the atmospheric O_3 content. Crutzen (*9*) reports that, with no N_2O in the atmosphere, the total atmospheric O_3 content would be 60 percent higher, whereas twice as much N_2O would yield 20 percent less atmospheric O_3.

However, since N_2O is produced at the earth's surface by denitrification and is then transported upward (*10*), the stratospheric N_2O abundance is determined by the N_2O mixing ratio at the tropopause. Tropospheric observations indicate that N_2O is well mixed with a residence time of 10 years or more (*11, 12*). Although tropospheric N_2O is destroyed by photodissociation (*10*), measurements of N_2O production in oceans and the temporal variability of N_2O concentrations (*11, 12*) suggest the existence of another unidentified, but dominant, tropospheric sink. (Our calculations include the effects of this unknown sink on the variability of N_2O.)

Although photolysis of N_2O is energetically possible for wavelengths below